JACS
JOURNAL OF THE AMERICAN CHEMICAL SOCIETY
Communication
pubs.acs.org/JACS

Energetics and Solvation Effects at the Photoanode/Catalyst Interface: Ohmic Contact versus Schottky Barrier

Yuan Ping,*[,†] William A. Goddard III,*[,†,‡] and Giulia A. Galli[§,∥]

[†]Joint Center for Artificial Photosynthesis, California Institute of Technology and Lawrence Berkeley National Laboratory, Berkeley, California 94720, United States

[‡]Materials and Process Simulation Center, California Institute of Technology, Pasadena, California 91125, United States

[§]Institute for Molecular Engineering, University of Chicago, Chicago, Illinois 60637, United States

[∥]Argonne National Laboratory, Lemont, Illinois 60439, United States

Supporting Information

ABSTRACT: The design of optimal interfaces between photoelectrodes and catalysts is a key challenge in building photoelectrochemical cells to split water. Iridium dioxide (IrO_2) is an efficient catalyst for oxygen evolution, stable in acidic conditions, and hence a good candidate to be interfaced with photoanodes. Using first-principles quantum mechanical calculations, we investigated the structural and electronic properties of tungsten trioxide (WO_3) surfaces interfaced with an IrO_2 thin film. We built a microscopic model of the interface that exhibits a formation energy lower than the surface energy of the most stable IrO_2 surface, in spite of a large lattice mismatch, and has no impurity states pinning the Fermi level. We found that, upon full coverage of WO_3 by IrO_2, the two oxides form undesirable Ohmic contacts. However, our calculations predicted that if both oxides are partially exposed to water solvent, the relative position of the absorber conduction band and the catalyst Fermi level favors charge transfer to the catalyst and hence water splitting. We propose that, for oxide photoelectrodes interfaced with IrO_2, it is advantageous to form rough interfaces with the catalyst, e.g., by depositing nanoparticles, instead of sharp interfaces with thin films.

Artificial photosynthesis, which uses photoelectrochemical cells (PECs) to split water into H_2 and O_2 or to reduce CO_2 to carbon fuels, is a promising strategy to produce clean and renewable energy.[1,2] The requirements for building efficient PEC are numerous and include (i) light absorbers with an optimal band gap for visible light absorption, (ii) efficient catalysts to assist the chemical reactions of water oxidation/reduction or CO_2 reduction, and (iii) interfaces between the absorber, catalyst, and water allowing for optimal charge transfer to the catalyst.

The oxygen evolution reaction (OER) is more complex than the hydrogen evolution reaction, involving four electrons instead of two. Iridium dioxide (IrO_2) is an efficient catalyst for OER and the only one known to be stable in acidic conditions.[4] Earth-abundant semiconductors stable in such conditions are also rare: tungsten trioxide (WO_3) is one of the few, with an acceptable optical gap of 2.6 eV.[1] Hence, using IrO_2 catalysts on WO_3 photoanodes is a promising strategy.[3] However, an important issue concerns the efficiency of the charge transfer from the absorber to the catalyst and then to water, so as to enable the oxidation process.

Recent experiments[3] showed that, in PECs, the photocurrents at WO_3/IrO_2 interfaces are much superior when IrO_2 is deposited on WO_3 through a sputtering method, which produces porous or nanostructured IrO_2, than when using spin-coating techniques, which lead to homogeneous IrO_2 crystalline layers. The reason for these different results obtained with the two preparation methods is yet unknown. Similarly, the low photocurrents obtained unexpectedly for several photoanodes[5] (e.g., Fe_2O_3) interfaced with IrO_2 remain unexplained.

In this Communication, we use first-principles calculations to provide insight into the properties of the WO_3/IrO_2 interface, and we interpret recent experiments;[3] we also define general criteria for optimal charge transfer between light absorbers and catalysts for the OER reaction that are general, and not restricted to pH conditions under which the reaction occurs.

Our investigation had three main objectives: (1) Derive a microscopic, energetically favorable model of the WO_3/IrO_2 interface, in spite of the large lattice mismatch. (2) Determine whether interfacial states are present, at a coherent interface, which might pin the Fermi level. (3) Interpret current experiments and provide guidance and design rules for future experiments interfacing IrO_2 with oxide photoelectrodes.

In the following, we describe how we tackled each of these problems, starting with the construction of a microscopic model of the interface. The lattice mismatch between WO_3 and IrO_2 is over 12%. We used first-principles calculations to search for a mismatched interface structure whose formation energy is lower than the surface energy of the constituent solids. The most stable stoichiometric surface of WO_3 is the (001)-c(2×2) reconstructed one, with a surface energy of 0.27 J/m^2 at the PBE level of theory (0.60 J/m^2 at PBE+D2); the most stable surface of IrO_2 is the (110) (rutile structure), with a surface energy of 1.44 J/m^2 within PBE (2.12 J/m^2 at PBE+D2). (A detailed comparison of surface energies of WO_3 and IrO_2 is presented in the Supporting Information (SI).)

Received: January 23, 2015
Published: April 13, 2015

DOI: 10.1021/jacs.5b00798
J. Am. Chem. Soc. 2015, 137, 5264−5267

We found that the geometry of room-temperature monoclinic WO_3 optimized using PBE+D2[6] is in much better agreement with experiments than the one obtained within PBE,[7] while the two methods yield only a 1% difference for the IrO_2 structure. (A detailed comparison of lattice constants of WO_3 and IrO_2 computed by different functionals is presented in the SI.) Hence, we relied on PBE+D2 geometries to compute interfacial and surface energy differences. Due to the high surface energy of IrO_2 compared to that of WO_3, we searched for an interface that stabilizes the IrO_2 surface. In particular, we stretched IrO_2 and compressed WO_3 laterally according to their corresponding bulk moduli (224 GPa for WO_3 and 266 GPa for IrO_2) so as to obtain the same pressure on both sides of our interface. We then fully optimized the internal geometry and cell parameters along the direction (z) perpendicular to the interface. By doing so, we obtained an interface energy ($\gamma = E_{\text{interface}} - E_{\text{bulk}}^{WO_3} - E_{\text{bulk}}^{IrO_2}$) of 1.27 J/m^2 at the PBE+D2 level of theory, much smaller than that of the most stable IrO_2 (110) surface; this indicates that the interface is energetically more stable than IrO_2 (110) in a vacuum. The stability of this interface is mainly attributed to two reasons: all interfacial Ir and W atoms are 6-fold coordinated, as in the bulk (i.e., Ir has a higher coordination than at the IrO_2 (110) surface), and no broken bonds are present at the interface.

The optimized atomic structure of the interface is shown in Figure 1; we verified that the electronic structure of the two bulk portions is well converged with respect to the number of atomic layers used in our model. This can be seen in Figure S3, where the planar average of the electrostatic potentials computed independently for bulk WO_3 and bulk IrO_2 coincides with that of the respective bulk regions of the interface model. We further investigated whether the electronic structures of bulk WO_3 and IrO_2 are modified when considering the lattice constant used to construct the interface (Figure 1), instead of the respective equilibrium lattice constants. Both the conduction band minimum (CBM) of WO_3 and the Fermi level (E_f) of IrO_2 were shifted to lower energy (−0.33 eV for WO_3 and −0.24 eV for IrO_2 at PBE+D2) compared with the values at equilibrium, which modified their *relative* alignment by less than 0.1 eV. In addition, we studied other interface geometries, e.g., (110)WO_3/(111)IrO_2 (see SI), which has the smallest lattice mismatch between the two materials (~2%); in this case we found an interface energy 0.65 J/m^2 higher than that of (001)WO_3/(110)IrO_2. However, the energy difference between the semiconductor CBM and the E_f of the (110)WO_3/(111)IrO_2 interface differed by only 0.13 eV from those of (001)WO_3/(110)IrO_2, which is the interface we discuss in detail below.

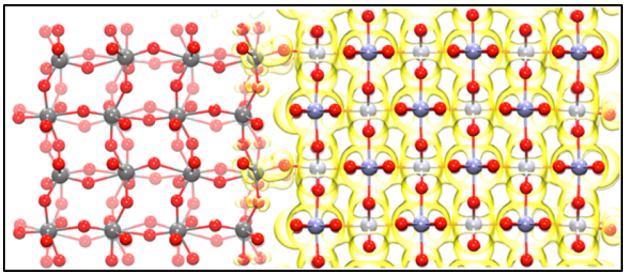

Figure 1. Crystalline (001)WO_3/(110)IrO_2 interface model (see text): the Ir, W, and O atoms are represented by ice blue, silver, and red spheres, respectively. Note that the O atoms at the IrO_2 (110) surface are bridge oxygens, each bonded to two Ir atoms. We also show the sum of square moduli of the wave functions (yellow isosurface) of single-particle states with energy inside the band gap of the WO_3 bulk region (as determined from local density of state calculations). The isosurface is 0.00308 e/bohr and includes 96% of the charge density.

Using the optimized interface model shown in Figure 1, we investigated whether interfacial states are present that may pin the interface Fermi level. Figure 1 also shows an isosurface of the density of the single-particle states with energy inside the band gap of crystalline WO_3. This isosurface is mostly localized within the IrO_2 region, with no significant components over the interface layers. This indicates that no extrinsic interfacial states (from defect states) are present to pin the Fermi level of the interface.

However, even in the absence of extrinsic states, the Fermi level could be pinned by so-called metal-induced gap states (MIGS): these are metal bulk states coupled to semiconductor evanescent states, with energies inside the band gap of the semiconductor. MIGS may pin the E_f of the interface at the semiconductor intrinsic charge neutrality level (CNL), as in the case of III−V semiconductor/metal interfaces.[8] The CNL is the first branch point of the complex band structure of the semiconductor.[9] To investigate whether the intrinsic MIGS are pinning the E_f of the interface, we computed the so-called Fermi level pining factor:[10,11] $S = 2/(1 + 0.1(\varepsilon_\infty - 1)^2)$, where ε_∞ is the high-frequency dielectric constant of the semiconductor. We obtained $S = 0.635$ for WO_3, much larger than the $S \approx 0$ value expected in the case of pinning (which is found, e.g., for some III−V semiconductor/metal interfaces[8]). This large S value stems from the ionic nature of WO_3, which has a significantly lower ε_∞ (5.63) than those of III−V semiconductors (10−16).

We computed the CNL of bulk WO_3 by the method proposed by Tersoff[8] and obtained $E_{\text{CNL}} = 0.80$ eV below the CBM of WO_3. We used a scissor operator to rigidly shift the conduction states and opened a band gap equal to that computed using many-body perturbation theory (precisely, using the GW approximation and geometries computed within DFT, at the PBE+D2 level of theory). The computed value of the CNL is closer to the CBM than the VBM, indicating that it is easier to dope WO_3 n-type than p-type.

In summary, our calculations showed that there are no defects or MIGS pinning the Fermi level of crystalline (001)WO_3/(110)IrO_2. Hence, for this system, the Schottky barrier height (SBH, φ_{SB}) at the interface depends on both the semiconductor band edge position and the Fermi level of the metal. The SBH is the key quantity determining the efficiency in separating majority electrons and minority holes at metal/semiconductor interfaces. If SBH is negative or close to zero, the majority electrons can easily flow through the interface and hence likely recombine with the minority holes, thus hampering photocurrents. By definition, interfaces with negative or close to zero SBH form Ohmic contacts.[9]

To calculate the SBH of the WO_3/IrO_2 interface, we first computed the relative position of the semiconductor band edges and the metal Fermi level. We used both PBE+D2 and many-body perturbation theory at the G_0W_0 level, with PBE+D2 wave functions (we call this level of theory G_0W_0@PBE+D2). We note that many-body perturbation theory led to good agreement with experimental photoemission data for WO_3 surfaces[13] and with the measured work function of the IrO_2 (110) surface (4.19 eV versus 4.23 eV in experiments;[14] see SI for details). We then obtained the SBH as $\varphi_{\text{SB}} = (E_{\text{CBM}} +$

DOI: 10.1021/jacs.5b00798
J. Am. Chem. Soc. 2015, 137, 5264−5267

$\Delta E_{CBM}^{GW}) - (E_F + \Delta E_F^{GW}) + \Delta V$, where ΔV is the difference of electrostatic potentials between bulk IrO_2 and WO_3 and the corresponding bulk regions in the interface model; $\Delta E_{F/CBM}^{GW}$ is the G_0W_0 correction to the eigenvalues of the individual bulk single-particle energies. We obtained $\varphi_{SB} = -0.32$ eV within DFT (PBE+D2) and −0.84 to −1.06 eV in many-body perturbation theory (G_0W_0@PBE+D2). The negative values of SBH indicate that the Fermi level of the interface is higher than the conduction band of WO_3, i.e., that the two oxides form an undesired Ohmic contact. This result is consistent with the experimental observation of Ohmic contacts when WO_3 is homogeneously coated with IrO_2 (e.g., by spin-coated deposition), as exemplified by the value of J_{back} (current density under back-illumination[15]) reported in ref 3. Hence, our calculations predicted that a perfect crystalline WO_3/IrO_2 interface does not favor charge transfer from the absorber to the catalyst.

If WO_3 is not homogeneously coated with IrO_2 so that a porous or nanostructured metal is present on the semiconductor, H_2O may penetrate the IrO_2 layer and be in direct contact with WO_3 (non-homogeneous coating is observed in experiments when using sputtering deposition methods[3]). In this case, to estimate the SBH, it is necessary to take into account the effect of water on the electronic structure of both the absorber and the catalyst. To do so, we used a solvation model[16] with one explicit water layer, and we predicted the solvation shift of the band edge positions of WO_3 and IrO_2 surfaces. We compared the stability between different water configurations on WO_3 and IrO_2 and computed the solvation shift for the most energetically stable surfaces.[17] For WO_3, we considered the presence of O vacancies at the surface[18] and obtained a solvation shift of 1.9−2.1 eV;[19] this shift accounts for the difference (1.9 ± 0.3 eV) between the position of the VBM of WO_3 inferred form electrochemical measurements[1,20] (which include the effect of solvent) and that measured by photoemission in ultrahigh vacuum[21,22] (where no solvent is present). In contrast, we found that the solvation shift of the work function of the IrO_2 surface is only 0.5−0.7 eV. Hence, the effect of solvent dramatically modifies the *relative* position of the CBM of WO_3 and the work function of IrO_2. This could possibly turn the intrinsic Ohmic contact between WO_3/IrO_2 into a Schottky barrier, as illustrated in Figure 2, which shows the main prediction of our study.[23]

Our results indicate that, in the absence of solvation effects, in order to obtain a favorable level alignment between the absorber and IrO_2, an absorber is required, with a CBM about 1 eV higher than that of WO_3. For example, Cu_2O has an optical gap of 1.95 eV[24] and an electron affinity of 3.2 eV, far above the WO_3 electron affinity of ∼6 eV[21,22] and also above the IrO_2 work function of 4.2 eV.[14] Hence, Cu_2O would appear to be a good candidate for a photoanode material to be interfaced with IrO_2. Instead, for many other oxides, including TiO_2, the position of the CBM is not favorable to form Schottky barriers with IrO_2. For example, in rutile TiO_2, the CBM is at −5.1 to −5.5 eV,[25] leading to Ohmic contacts. However, our calculations and experimental results indicate that solvation effects shift the band edge positions of rutile TiO_2 by ∼1.0 eV.[17,26] Hence, we predict that using porous or nanostructured IrO_2 can possibly improve the charge transfer also for TiO_2, similar to the case of WO_3 shown in Figure 2.

Summarizing, we showed that, in the case of the WO_3/IrO_2 interface, homogeneous coatings of the photoanode results in an undesirable Ohmic contact. However, we predicted that partial water exposure of both oxides may favor the transfer of holes from the anode to the catalyst, a necessary step for the OER to occur. We suggest that formation of a rough interface would expose both oxides to water and lead to a favorable alignment of the semiconductor conduction band and the metal work function. In particular, our first-principles calculations showed that, upon water exposure, the energy difference between the light absorber CBM and the Fermi energy of the interface may change sign, thus converting Ohmic contacts to Schottky barriers. It is this energy difference, in the presence of the solvent, that can be optimized for best performance of PEC, e.g., with rough absorber/catalyst interfaces.

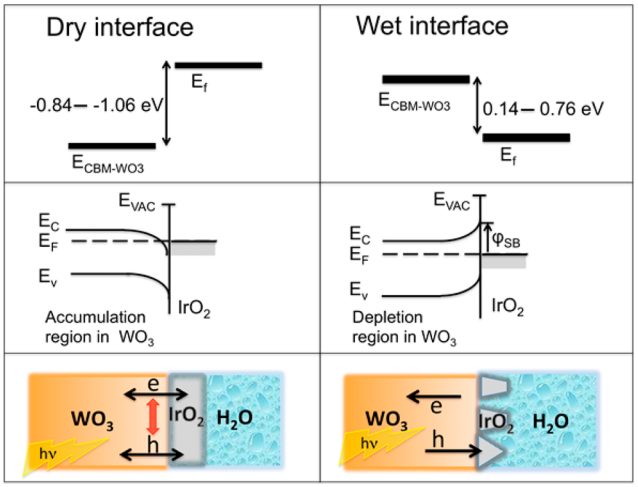

Figure 2. Relative position of the conduction band minimum of WO_3 (E_{CBM}) and the Fermi level (E_f) of the interface, in the absence of water (left panel), and in the presence of water in contact with the absorber and the catalyst at the same time (right panel). We show results obtained at the G_0W_0@PBE+D2 level of theory (see text; the corresponding ones at the PBE+D2 level are −0.32 eV in the absence of water and 0.88−1.28 eV in the presence of water). We estimated the numerical inaccuracies of the many-body perturbation theory results to be ∼ −0.2 eV for the Fermi level of IrO_2 and 0.05 eV for the CBM of WO_3 (see SI); we indicated those errors by thick lines. The solvation shift of IrO_2 (WO_3) has a range of 0.5−0.7 (1.9−2.1) eV, depending on the water configuration at the surface; therefore, we used thick lines to represent results in the presence of water. We also show a cartoon representation of the band-bending in the semiconductor in the case of Ohmic contacts (left panel) and Schottky barriers (right panel).

■ ASSOCIATED CONTENT

Supporting Information

Computational details of DFT and G_0W_0 calculations; surface energy and band alignment. This material is available free of charge via the Internet at http://pubs.acs.org.

■ AUTHOR INFORMATION

Corresponding Authors

*yping@lbl.gov
*wag@wag.caltech.edu

Notes

The authors declare no competing financial interest.

■ ACKNOWLEDGMENTS

We thank Ravishankar Sundararaman, Francois Gygi, Joshua Spurgeon, Alessandro Fortunelli, Hai Xiao, Ding Pan, and Tuan Anh Pham for useful discussions. This paper is based on work

DOI: 10.1021/jacs.5b00798
J. Am. Chem. Soc. 2015, 137, 5264−5267

performed at the Joint Center for Artificial Photosynthesis, a DOE innovation hub, supported through the Office of Science of the U.S. Department of Energy under Award No. DE-SC0004993. G.A.G. acknowledges support from Argonne National Laboratory under U.S. Department of Energy contract DE-AC02-06CH11357.

REFERENCES

(1) Walter, M. G.; Warren, E. L.; McKone, J. R.; Bottcher, S. W.; Mi, Q. X.; Santori, E. A.; Lewis, N. S. *Chem. Rev.* **2010**, *110*, 6446.
(2) Kumar, B.; Llorente, M.; Froehlich, J.; Dang, T.; Sathrum, A.; Kubiak, C. P. *Annu. Rev. Phys. Chem.* **2012**, *63*, 541.
(3) Spurgeon, J. M.; Velazquez, J. M.; McDowell, M. T. *Phys. Chem. Chem. Phys.* **2014**, *16*, 3623.
(4) McCrory, C. C.; Jung, S.; Peters, J. C.; Jaramillo, T. F. *J. Am. Chem. Soc.* **2014**, *136*, 16104.
(5) Badia-Bou, L.; Mas-Marza, E.; Rodenas, P.; Barea, E. M. *J. Phys. Chem. C* **2013**, *117*, 3826.
(6) Grimme, S. *J. Comput. Chem.* **2006**, *27*, 1787.
(7) Ping, Y.; Li, Y.; Gygi, F.; Galli, G. *Chem. Mater.* **2012**, *24*, 4252.
(8) Tersoff, J. *Phys. Rev. Lett.* **1984**, *52*, 465.
(9) Lüth, H. *Solid surfaces, interfaces and thin films*; Springer: Berlin, 2001.
(10) Monch, W. *Phys. Rev. Lett.* **1987**, *58*, 1260.
(11) Dag, S.; Wang, L. W. *Phys. Rev. B* **2010**, *82*, 241303.
(12) Ping, Y.; Rocca, D.; Galli, G. *Phys. Rev. B* **2013**, *87*, 165203.
(13) Ping, Y.; Galli, G. *J. Phys. Chem. C* **2014**, *118*, 6019.
(14) Chalamala, B. R.; Wei, Y.; Reuss, R. H.; Aggarwal, S.; Gnade, B. E. *Appl. Phys. Lett.* **1999**, *74*, 1394.
(15) The sputtering method gives much higher current density (0.90−0.91 mA/cm^2) than the spin-coated one (0.71−0.17 mA/cm^2). We also note that, when the thickness of the IrO_2 film is increased by sputtering, J_{back} remains unchanged; however, when the thickness of spin-coated IrO_2 is increased, the current density drops dramatically from 0.71 (with 1 coat ∼1nm) to 0.17 within two coats. Hence, the interface of spin-coated WO_3/IrO_2 is much less efficient than the one obtained by sputtering.
(16) Sundararaman, R.; Goddard, W. A. *J. Chem. Phys.* **2015**, *142*, 064107.
(17) Ping, Y.; Sundararaman, R.; Galli, G.; Goddard, W., *manuscript in preparation*, 2015.
(18) We considered O vacancies when WO_3 is in direct contact with water, as in this case water molecules can bind to the O vacancy sites, i.e., to W atoms with dangling bonds, thus effectively lowering the vacancy formation energy. However, in the case of a homogeneous interface between WO_3 and IrO_2, the presence of O vacancies (i.e., W dangling bonds) would lead to an increase of the interface energy and thus to vacancy formation energies much more energetically unfavorable than in case of the wet surface.
(19) The variation of the solvation shift (∼0.2 eV) mainly stems from the presence, at finite temperature, of hydroxyl-terminated surface atoms, coexisting with configurations in which water molecules are not dissociated. Different water configurations give rise to different surface dipoles.
(20) Yourney, J.; Bartlett, B. *J. Mater. Chem.* **2011**, *21*, 7651.
(21) Meyer, J.; Kroger, M.; Hamwi, S.; Gnam, F.; Riedl, T.; Kowalsky, W.; Kahn, A. *Appl. Phys. Lett.* **2010**, *96*, 193302.
(22) Kroger, M.; Hamwi, S.; Meyer, J.; Riedl, T.; Kowalsky, W.; Kahn, A. *Appl. Phys. Lett.* **2009**, *95*, 123301.
(23) We note that measurements performed in air instead of solution (see ref 3) show that sputtered IrO_2 on WO_3 forms an Ohmic contact, similar to the case of the spin-coated WO_3/IrO_2 interface. This shows that it is indeed the effect of water to make the sputtered WO_3/IrO_2 interface a rectifying Schottky barrier.
(24) Jeong, S. S.; Mittiga, A.; Salza, E.; Masci, A.; Passerini, S. *Electrochim. Acta* **2008**, *53*, 2226.
(25) The electron affinity of TiO_2 was obtained from the photoemission measurements of the VBM plus the experimental photoemission band gap of rutile TiO_2 from ref 22.
(26) Onda, K.; Li, B.; Petek, H. *Phys. Rev. B* **2004**, *70*, 045415. Gratzel, M. *Nature* **2001**, *414*, 338.

DOI: 10.1021/jacs.5b00798
J. Am. Chem. Soc. 2015, 137, 5264−5267